Journal of Geoscience and Environment Protection, 2026, 14(10), 388-403
https://www.scirp.org/journal/gep
ISSN Online: 2327-4344
ISSN Print: 2327-4336

Chemical Characteristics of Precipitation and Its Effects on Atmospheric Pollutants in Suburban Areas of Cangzhou, China

Jian Wang[1], Sisi Li[1], Yanan Zhao[1], Yufeng Mao[1], Na Mao[2], Qingshui Yu[1], Wenyu Zhang[1], Cuihua Zhang[1], Mei Xu[1*]

[1]College of Chemistry and Chemical Engineering, Cangzhou Normal University, Cangzhou, China
[2]Cangzhou Municipal Research Institute of Environmental Protection, Cangzhou, China
Email: *xm308@163.com

How to cite this paper: Wang, J., Li, S. S., Zhao, Y. N., Mao, Y. F., Mao, N., Yu, Q. S., Zhang, W. Y., Zhang, C. H., & Xu, M. (2026). Chemical Characteristics of Precipitation and Its Effects on Atmospheric Pollutants in Suburban Areas of Cangzhou, China. *Journal of Geoscience and Environment Protection, 14,* 388-403.
https://doi.org/10.4236/gep.2026.1410016

Received: September 15, 2026
Accepted: October 27, 2026
Published: October 30, 2026

Copyright © 2026 by author(s) and Scientific Research Publishing Inc.
This work is licensed under the Creative Commons Attribution International License (CC BY 4.0).
http://creativecommons.org/licenses/by/4.0/
Open Access

Abstract

Observations of precipitation chemistry and major atmospheric pollutant mass concentrations in suburban Cangzhou in 2021 were used to characterize regional precipitation chemistry. Precipitation measurements included pH, electrical conductivity, and water-soluble ion concentrations. Pollutant variations were compared between rainy days and non-rainy days. The observed pH range of 6.18 - 8.02 and volume-weighted mean of 6.71 suggested that precipitation in the study area was not acidified during the sampling period. The electrical conductivity ranged from 6.85 to 290 μS/cm, and the volume-weighted mean was 40.29 μS/cm. The total ion concentrations ranged from 86.14 to 3221.58 μeq/L, with a volume-weighted mean of 366.13 μeq/L. Ca^{2+} and NH_4^+ were the dominant cations, accounting for 46.82% and 25.33% of the total cation concentration, respectively. NO_3^- and SO_4^{2-} were the principal anions, accounting for 45.57% and 40.08% of the total anion concentrations, respectively. On rainy days, mass concentrations of $PM_{2.5}$, PM_{10}, SO_2, NO_2, and CO were lower than those on non-rainy days by 27.97%, 40.62%, 27.32%, 25.36%, and 17.78%, respectively. These differences demonstrated that the scavenging effect by precipitation varied among atmospheric pollutants and was most pronounced for PM_{10}. The regulatory effects of precipitation differed among atmospheric pollutants. Together with improved atmospheric dispersion, wet deposition effectively reduced $PM_{2.5}$, PM_{10}, NO_2, SO_2, and CO concentrations, with PM_{10} and SO_2 being the most sensitive to rain. Conversely, the increase in O_3 concentrations on rainy days was attributed to changes in atmospheric composition and solar radiation conditions.

Keywords

Atmospheric Particles, Atmospheric Precipitation, Scavenging Effect, Chemical Composition

1. Introduction

As an important route of air pollutant removal, atmospheric precipitation can transport gaseous and particulate pollutants to the ground through in-cloud scavenging and below-cloud washout (Chen et al., 2025a; Sun et al., 2025). The geochemical cycling of terrestrial elements is substantially altered by the diverse chemical constituents of precipitation, with profound consequences for terrestrial ecosystems (Zeng et al., 2024). Analyses of precipitation chemistry enable researchers to characterize air pollutant composition and temporal variability and trace potential pollutant sources (Si & Li, 2024). The chemical constituents of precipitation can indicate the degree and state of atmospheric pollution while providing a fundamental basis for examining changes in atmospheric composition and the effects of human activities on the atmospheric environment (Huang et al., 2024). Therefore, investigating precipitation chemistry and its interactions with air pollutants is of considerable importance.

Research in China has extensively examined the chemical composition, spatiotemporal distribution, and sources of atmospheric precipitation, as well as the factors governing pollutant removal by precipitation. In Harbin, a megacity in northeastern China, Chen et al. (2025a) collected 99 precipitation samples between November 2021 and October 2023. They measured pH and the concentrations of major water-soluble ions, including Na^+, K^+, Ca^{2+}, Mg^{2+}, NH_4^+, NO_3^-, SO_4^{2-}, Cl^-, and F^-. By analyzing long-term precipitation monitoring records from Beijing for 1997-2020, Sun et al. (2021) identified an abrupt shift in precipitation pH in 2008. Specifically, a generally downward trend during 1997-2008 was followed by a gradual rise. Sulfate and nitrate predominated among the anions, and their concentrations decreased overall. Using precipitation samples collected at three monitoring sites in Guilin during 2013-2017, Li et al. (2020a) characterized precipitation chemistry and the contributions of different ion sources against a background of reduced air pollutant levels. In Weinan, a key city on the Guanzhong Plain, Sun et al. (2025) examined the relationship between local precipitation chemistry and meteorological and environmental factors. The sample composition was systematically interpreted using chemometric and correlation analyses, positive matrix factorization, and backward trajectory modeling. Using pollutant concentration and precipitation records from Dalian, Chen et al. (2025b) conducted an in-depth investigation of gaseous pollutant scavenging with respect to precipitation amount, monthly variation, and initial concentration. Situated in southeastern Hebei Province at the center of the Bohai Rim region, Cangzhou has a favorable geographical location. Nevertheless, few recent studies have addressed atmospheric precipita-

tion and its scavenging effects in this region (Wang et al., 2022; Xiong et al., 2021). To address this gap, the present study used 2021 observations of precipitation chemistry and major atmospheric pollutant mass concentrations in Cangzhou. The precipitation measurements included pH, electrical conductivity, and water-soluble ion concentrations. These data were used to characterize precipitation chemistry and compare pollutant variations between precipitation and non-precipitation periods. This study emphasized the influence of precipitation on atmospheric pollutants and aimed to provide a scientific basis for regional air pollution control.

2. Materials and Methods

2.1. Sample Collection and Analysis

The sampling site was the roof of a bungalow on the campus of Cangzhou Normal University in Cangzhou, with no nearby tall buildings or typical pollution sources. Precipitation was collected using an SYC-3 refrigerated precipitation-dust sampler (Qingdao Laoshan Electronic Instrument General Factory Co., Ltd., China) from February to December 2021. Samples were collected every 24 h, with each sampling period defined as 8:00 on the current day to 8:00 on the next day. A total of 48 mixed precipitation samples were obtained. The collected precipitation samples were stored in 50 mL polyethylene bottles and preserved by freezing. According to weather forecasts, for precipitation events with heavy precipitation amounts and long duration, stage-based sampling was conducted using a precipitation volume threshold of 100 mL. Since the instrument can hold a maximum of eight sampling bottles at one time, up to eight staged samples could be collected for a single precipitation event, which were labelled as Stage 1, Stage 2, Stage 3, Stage 4, Stage 5, Stage 6, Stage 7 and Stage 8. The Stage 8 sample was collected until the end of the daily precipitation event, and the volume was calculated based on the actual precipitation volume. Three precipitation events were sampled in this study, occurring on July 7, July 31, and October 6, 2021, with 7, 8, and 8 corresponding samples, respectively. Before each sampling event, the collection bucket was rinsed with ultrapure water to prevent cross-contamination between precipitation samples.

Measurements comprised pH, electrical conductivity, and water-soluble ion concentrations (Na^+, NH_4^+, K^+, Mg^{2+}, Ca^{2+}, Cl^-, NO_3^-, and SO_4^{2-}). The pH and electrical conductivity were determined using a P611 pH meter and a P612 conductivity meter, respectively (Youke Instrument Co., Ltd., Shanghai, China). Prior to measurement, the pH meter was calibrated with standard buffer solutions at pH 4.00, 6.86, and 9.73, and the conductivity meter was calibrated using a standard solution with an electrical conductivity of 1408 μs/cm. Following filtration through 0.45 μm microporous membranes, water-soluble ion concentrations were determined using an Aquion ion chromatograph (Thermo Fisher Scientific, USA). Anions were measured using an AS19 analytical column, an AG19 guard column, and an AERS 600 suppressor with 20 mmol/L KOH eluent. Cations were analyzed using a CS12A analytical column, a CG12A guard column, and a CERS 600 sup-

pressor with 20 mmol/L methanesulfonic acid eluent. The flow rate was 1 mL/min, and the injection volume was 25 μL for both anion and cation analyses, using a conductivity detector. Water-soluble ion concentrations were quantified by the external standard calibration curve method. Six concentration gradients were established for each ion. Within the corresponding linear ranges, the R^2 values of the calibration curves for all ions were greater than 0.995, showing good linearity. Before sample analysis, the performance of the analytical instrument was optimized to improve measurement sensitivity and resolution and ensure data accuracy.

2.2. Data Processing and Quality Assurance

Mass-concentration data of atmospheric pollutants during the study period were obtained from the Tianqihoubao website, including $PM_{2.5}$, PM_{10}, SO_2, NO_2, O_3, and CO. Rainy days and non-rainy days were defined according to whether precipitation occurred during sampling. The mass concentrations of atmospheric pollutants on rainy days (48 d) and non-rainy days (317 d) were then calculated to analyze the effects of precipitation on atmospheric pollutants. To reduce potential biases caused by ion molar mass and valence on ion concentrations, ion equivalent concentration (μeq/L) was adopted instead of ion mass concentration. Based on the measurements of various precipitation samples, the volume-weighted method was used to calculate pH, electrical conductivity, and water-soluble ion concentrations of precipitation samples collected during the sampling period (Li et al., 2020b; Zhang, 2013). Notably, the mean precipitation pH was statistically derived from volume-weighted hydrogen ion concentrations. Precipitation parameters and atmospheric pollutant mass concentrations were organized and subjected to statistical analysis using Microsoft Excel 2016. Column charts, line graphs, and other figures were prepared using Origin 8.5. These analyses were used to further examine regional precipitation chemistry and the effects of precipitation on the atmospheric pollutants.

The anion-cation equivalent balance is an important indicator for assessing the representativeness of ions in precipitation and ensuring data quality. The anion/cation equivalent ratio obtained in this study was 0.71, where anions showed slightly lower equivalent concentrations than cations. This discrepancy was likely caused by unmeasured species, including F^-, NO_2^-, HCO_3^-, CO_3^{2-}, PO_3^{3-} and several low-molecular-weight organic acid anions (Xiao et al., 2024). The R^2 between total anion and cation equivalents was 0.87, demonstrating strong correlations among Na^+, NH_4^+, K^+, Mg^{2+}, Ca^{2+}, Cl^-, NO_3^-, and SO_4^{2-}. These ions are highly representative and are the primary water-soluble ions in precipitation, supporting the reliability of our data. Electrical conductivity acts as a comprehensive indicator of total water-soluble ion content. A strong correlation (R^2 = 0.96) existed between precipitation electrical conductivity and total ion equivalent concentration, further confirming the accuracy and validity of the ion and conductivity measurements.

3. Results and Discussion

3.1. pH and Electrical Conductivity of Precipitation

The observed precipitation pH range in the study area was 6.18 - 8.02, and the volume-weighted mean over the sampling period was 6.71. With all values above the acid rain threshold of pH 5.6, the results indicated no precipitation acidification and no adverse effects on environmental acidification. The relatively elevated pH may be associated with high Ca^{2+} concentrations in the study area (**Figure 1**). Representing 27.32 % of the total ion concentration, Ca^{2+} has a strong capacity to buffer precipitation acidity (Xiao et al., 2015). Compared with the values reported in earlier studies in northern China, the volume-weighted mean pH was higher than that in Shijiazhuang (6.10) (Hong et al., 2014) and Beijing (6.00) (Yang et al., 2012). The study mean was comparable to that in Tianjin (6.68) (Yang et al., 2023) and Xi'an (6.64) (Lu et al., 2011) and lower than that in Lanzhou (7.70) (Xu et al., 2009) and Qinghai (7.10) (Zhang et al., 2003). The generally high precipitation pH in northern China is primarily associated with neutralization by local alkaline soils. Compared with southern Chinese sites, pH in the study area was markedly higher than that in Hangzhou (4.65) (Wu et al., 2021b), Wuxi (5.88) (Wang et al., 2021), and Shenzhen (5.12) (Huang et al., 2024). The clear spatial variation in precipitation pH across China is characterized by greater acidity in the south and a stronger neutralization potential in the north (Huang & Li, 2024).

3.2. Chemical Composition of Precipitation

Across precipitation samples, total ion concentrations ranged from 86.14 to 3221.58 μeq/L. Their volume-weighted mean of 366.13 μeq/L considerably exceeded the value of 142.5 μeq/L recorded at the Waliguan Mountain atmospheric background station (Tang et al., 2000). The classification proposed by Cheng and Huang (1998) divides precipitation into five pollution grades according to total ion concentration: clean (≤100 μeq/L), slightly polluted (100 - 300 μeq/L), moderately polluted (300 - 500 μeq/L), heavily polluted (500 - 1000 μeq/L), and extremely polluted (≥1000 μeq/L). The samples in these five grades accounted for 2.08% (1), 31.25% (15), 16.67% (8), 20.83% (10), and 29.17% (14) of all samples collected during the sampling period, respectively. The slightly and extremely polluted categories contained the largest sample proportions. The volume-weighted mean total ion concentration categorized the precipitation in the study area as moderately polluted. These results reveal substantial regional atmospheric pollution that warrants close attention.

Figure 1 presents the volume-weighted concentrations of individual precipitation ions over the sampling period, showing significant differences among ions. Total cation concentrations ranged from 50.78 to 1776.27 μeq/L and had a volume-weighted mean of 213.64 μeq/L. Cation composition was dominated by Ca^{2+} and NH_4^+, with concentrations ranging from 11.34 to 1120.08 μeq/L and from

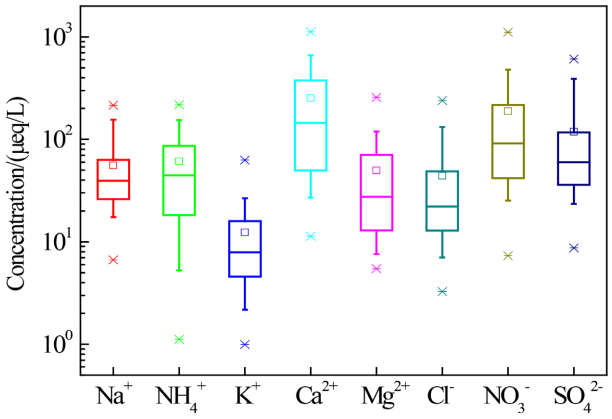


Figure 1. Volume-weighted concentrations of different water-soluble ions in precipitation.

1.12 to 218.09 μeq/L, respectively. Their volume-weighted means of 100.03 and 54.12 μeq/L represented 46.82% and 25.33% of the total cation concentrations, respectively. The total anion concentrations ranged from 35.37 to 1742.83 μeq/L, with a volume-weighted mean of 152.50 μeq/L. NO_3^- and SO_4^{2-} were the dominant anions. Their concentrations ranged from 7.31 to 1112.89 μeq/L and 8.71 to 609.88 μeq/L, respectively. The corresponding volume-weighted means were 69.50 and 61.12 μeq/L. These ions contributed 45.57% and 40.08% of the total anions, respectively. Accordingly, sulfate and nitrate were the principal acid-forming substances in the study area. The volume-weighted ion concentrations followed the order $Ca^{2+} > NO_3^- > SO_4^{2-} > NH_4^+ > Na^+ > Cl^- > Mg^{2+} > K^+$. Together, the volume-weighted concentrations of Ca^{2+}, NO_3^-, SO_4^{2-}, and NH_4^+ represented 77.78% of the total ion concentration, making them the dominant ions in local precipitation. This pattern was generally consistent with precipitation chemistry elsewhere in northern China (Hou et al., 2020; Xiao et al., 2015). In addition, the ratio of $([Ca^{2+}] + [NH_4^+])$ to $([NO_3^-] + [SO_4^{2-}])$ exceeded 1. This suggests that carbonic acid and other organic acids, along with NO_3^- and SO_4^{2-}, also influence precipitation acidity in Cangzhou (Hou et al., 2020).

3.3. Variations in Chemical Composition during Precipitation Events

Stage-based examination of precipitation events can capture real-time changes in chemical constituent concentrations and further reveal how precipitation scavenges atmospheric pollutants (Han et al., 2017). **Figure 2** illustrates the changes in the total water-soluble ion concentrations during three typical precipitation events, on July 7, July 31, and October 6, 2021. The respective concentration ranges were 244.01 - 629.85, 177.07 - 382.33, and 42.43 - 380.07 μeq/L, with variation amplitudes of 385.83, 205.26, and 337.64 μeq/L. For both July 7 and July 31, the highest total ion concentration occurred at the onset of precipitation (the first stage), after which the concentrations fell rapidly and eventually stabilized with precipitation. On October 6, the concentrations increased in the second stage before gradually declining and stabilizing toward the end of the event. These patterns

indicate high atmospheric pollutant levels at the onset of precipitation. The large quantities of pollutants washed into rainwater resulted in high ion concentrations during the initial precipitation. As precipitation continued, atmospheric pollutant loads decreased, and below-cloud scavenging gradually weakened. Consequently, the decline in ion concentrations was followed by relatively low and stable concentrations in the later stages of precipitation.

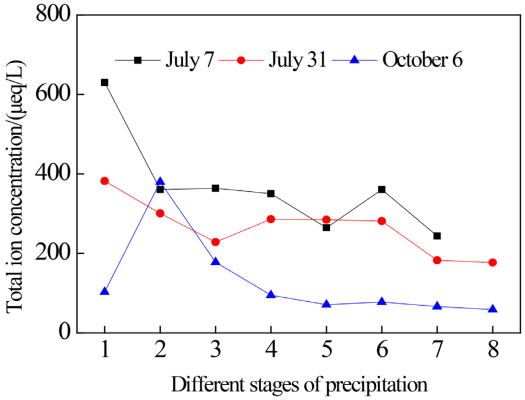


Figure 2. Volume-weighted total concentrations of water-soluble ions for typical precipitation events.

Figures 3-5 present the volume-weighted concentrations of individual water-soluble ions at successive stages of the three typical events on July 7, July 31, and October 6, respectively. The variation patterns differed among water-soluble ions over the course of precipitation. In **Figure 3**, the extremely high initial Ca^{2+} concentration during the July 7 event (stage 1) was followed by a rapid decrease and an overall downward trend, despite subsequent minor fluctuations. This pattern can be explained by the ease with which rainwater scavenges coarse Ca-containing particles (e.g., dust) at the onset of precipitation. As precipitation continued, these coarse particles became less abundant, resulting in a gradual decrease in Ca^{2+} concentration. Marked fluctuations in NH_4^+ concentrations, with no obvious downward trend, suggest complex sources. Its concentration

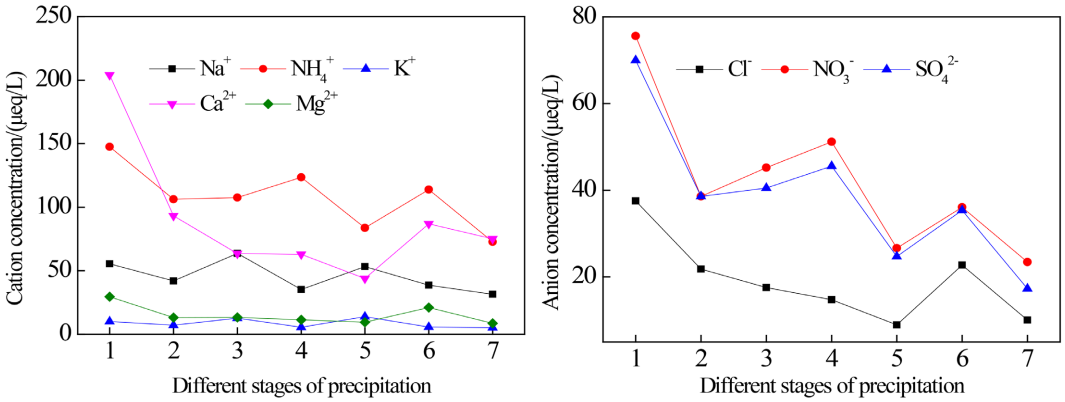


Figure 3. Volume-weighted mean concentrations of water-soluble ions during the typical precipitation event on July 7.

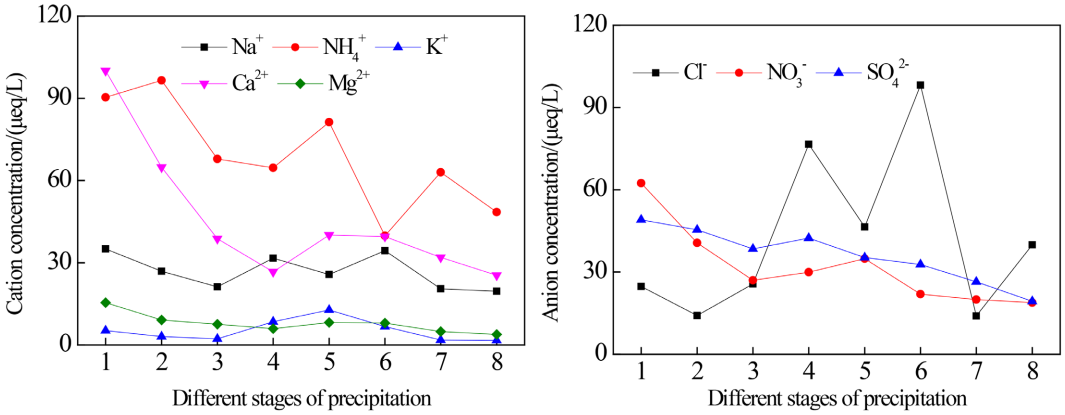


Figure 4. Volume-weighted mean concentrations of water-soluble ions during the typical precipitation event on July 31.

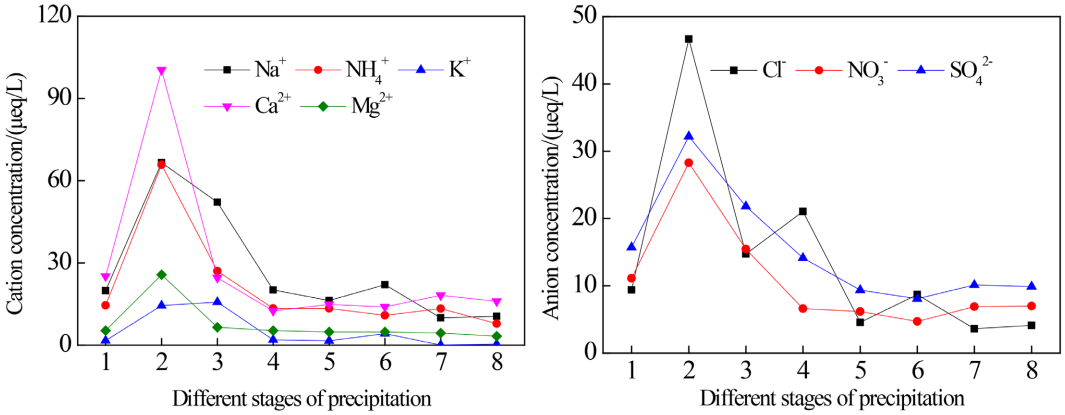


Figure 5. Volume-weighted mean concentrations of water-soluble ions during a typical precipitation event on October 6.

varied across precipitation stages under the combined influence of atmospheric ammonia emissions and secondary transformation of other substances. Throughout the event, Na^+, Mg^{2+}, and K^+ concentrations remained relatively low and varied only slightly, indicating the lower susceptibility of these ions to rain scavenging. NO_3^- and SO_4^{2-} exhibited similar variation patterns. Their concentrations peaked in Stage 1, fell sharply, and then rebounded slightly with fluctuations before declining overall. The intensive initial scavenging of nitrogen- and sulfur-containing pollutants accounted for the high concentrations at the beginning of precipitation. Subsequent fluctuations were likely caused by the replenishment of relevant pollutants through atmospheric chemical reactions. For Cl^-, the concentrations decreased steadily from the initial to final stages of precipitation.

Compared with the July 7 event, similar variation patterns were evident on July 31 and October 6 (Figure 4 & Figure 5). Ca^{2+} and NH_4^+ were the predominant cations. Ca^{2+} concentrations peaked early and then gradually decreased over the precipitation events, with slight synchronous rebounds at certain intervals. NH_4^+ concentrations fluctuated throughout the events without a monotonic trend. Overall, they were relatively high in the early stages and declined slowly in the later stages.

Na^+, Mg^{2+}, and K^+ contributed small proportions and varied only mildly during precipitation. The anions NO_3^- and SO_4^{2-} were initially high and subsequently decreased gradually, with minor fluctuations. The comparison of Figures 3-5 demonstrates evident differences among the three events. Most ions peaked at Stage 1 on July 7 and July 31, whereas their maximum was identified at Stage 2 on October 6. Moreover, NH_4^+ and Cl^- exhibited different variation patterns. On July 7, NH_4^+ fluctuated gently at moderate to high levels. On July 31, it declined with more intense fluctuations and frequent alternations between high and low concentrations. On October 6, a pronounced peak occurred only at Stage 2, with stable and low concentrations in the other stages. Furthermore, Cl^- decreased steadily from the beginning to the end of the precipitation on July 7, with negligible fluctuations. On July 31, large fluctuations produced multiple peaks, including several high concentrations during the middle and late stages. During the October 6 event, the concentrations rose and fell to form a single peak, whereas the intensity of their fluctuations lay between those of the other two events.

3.4. Effects of Precipitation on Atmospheric Pollutants

Particulate matter with aerodynamic diameters of ≤2.5 and ≤10 μm is denoted as $PM_{2.5}$ and PM_{10}, respectively. Figure 6 compares rainy and non-rainy days in terms of the mass concentrations of major air pollutants ($PM_{2.5}$, PM_{10}, SO_2, NO_2, O_3, and CO) and their rates of concentration change. As shown in Figure 6, mean $PM_{2.5}$ concentrations were 30.41 μg/m³ on rainy days and 42.21 μg/m³ on non-rainy days. The corresponding PM_{10} concentrations were 50.15 and 84.47 μg/m³. The reported reductions were 27.97% for $PM_{2.5}$ and 40.62% for PM_{10}. These lower particulate matter concentrations observed on precipitation days indicate an association between precipitation and pollutant levels. (Luan et al., 2021). The greater reduction in PM_{10} than in $PM_{2.5}$ indicates more efficient removal of coarse particles. Because larger particles can collide more efficiently with raindrops, their

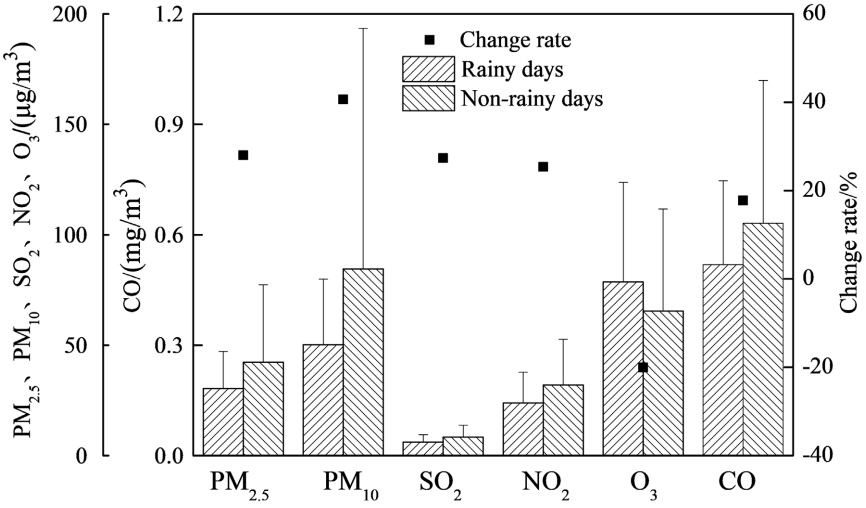


Figure 6. Mass concentrations of atmospheric pollutants and their rates of change on rainy and non-rainy days.

scavenging is more effective (Wu et al., 2021a). Other gaseous pollutants, except O_3, exhibited similar decreases. SO_2 concentrations fell from 8.43 μg/m³ on non-rainy days to 6.13 μg/m³ on rainy days, NO_2 from 31.93 to 23.83 μg/m³, and CO from 0.63 to 0.52 mg/m³. The corresponding reductions were 27.32%, 25.36%, and 17.78%, respectively. Precipitation can scavenge gaseous pollutants, although less effectively than PM_{10}. Studies in the coastal city of Dalian have reported rainy-day reductions of 36.5% for SO_2 and 29.6% for NO_2 (Chen et al., 2025b). Similarly, research in Guiyang, southwestern China, verified the general scavenging effect of precipitation on air pollutants, with a more pronounced removal of particulate matter, particularly PM_{10} (Zeng et al., 2021). A study conducted in Chongqing, a mountainous city in southwestern China, demonstrated that summer precipitation generally has a strong scavenging effect on PM_{10} and SO_2, regardless of precipitation intensity, duration, or cumulative amount. Its effect on O_3 was limited. This difference is attributed to the high water solubility of PM_{10} and SO_2 and the low water solubility of O_3, which results in a negligible O_3 scavenging effect by precipitation (Wang et al., 2017). Accordingly, both precipitation characteristics and the intrinsic properties of pollutants are associated with the scavenging efficiency of precipitation for air pollutants.

3.5. Diurnal Variations in Atmospheric Pollutant Concentrations on Rainy and Non-Rainy Days

Figure 7 presents the diurnal changes in $PM_{2.5}$ and PM_{10} concentrations and the $PM_{2.5}/PM_{10}$ ratio on rainy and non-rainy days. On non-rainy days, $PM_{2.5}$ and PM_{10} concentrations ranged from 34.3 to 47.4 μg/m³ and from 77.5 to 94.2 μg/m³, respectively, with both displaying typical morning and evening peaks of a bimodal

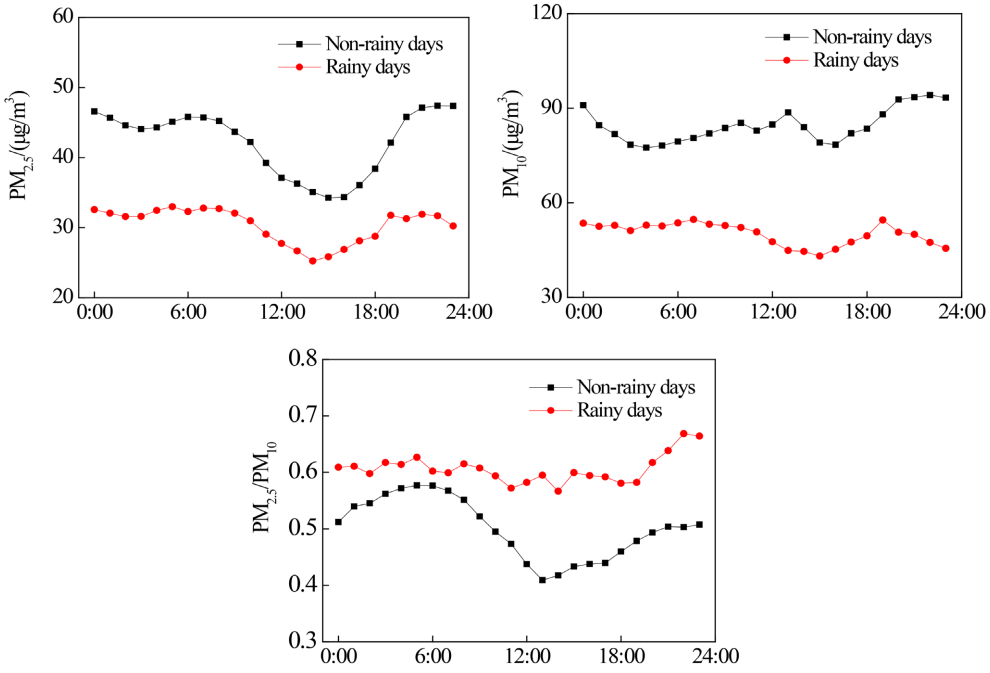


Figure 7. Diurnal variations in $PM_{2.5}$ and PM_{10} mass concentrations and the $PM_{2.5}/PM_{10}$ ratio on rainy and non-rainy days.

pattern. During the early morning and morning hours, and from evening into the night, poor atmospheric dispersion favorednear-surface accumulation of particulate matter and sustained high concentrations. At midday, atmospheric dispersion improved as convection intensified, whereas particulate matter concentrations gradually declined, with distinct differences between intraday peaks and troughs. The $PM_{2.5}/PM_{10}$ ratio ranged from 0.41 to 0.58 and fluctuated considerably. The midday decrease indicated that coarse particles accounted for a relatively larger proportion at that time.

On rainy days, the $PM_{2.5}$ and PM_{10} concentrations were 25.2 - 33.0 and 43.1 - 54.5 μg/m^3, respectively, generally below those on non-rainy days. This demonstrates the effective removal of atmospheric particles by wet deposition during precipitation. For $PM_{2.5}$ and PM_{10}, diurnal variation amplitudes were 13.1 and 16.7 μg/m^3 on non-rainy days, versus 7.41 and 11.4 μg/m^3 on rainy days. The smaller range on rainy days suggests that in addition to lowering absolute particle concentrations, precipitation dampens diurnal fluctuations. Under continuous wet scavenging, the original bimodal diurnal pattern disappeared. Particle concentrations remained stable throughout the day, with markedly reduced fluctuations. The rainy-day $PM_{2.5}/PM_{10}$ ratio of 0.57 - 0.67 revealed a clear increase in the proportion of fine particles. This may be related to either less efficient scavenging of fine particles by raindrops or secondary aerosol formation after precipitation.

Figure 8 shows the diurnal patterns of NO_2, SO_2, O_3, and CO concentrations on rainy and non-rainy days. Typical diurnal fluctuations were evident for all pollutants during non-rainy conditions. NO_2 concentrations ranged from 17.7 to 40.8 μg/m^3, with morning and evening peaks forming a bimodal pattern. Rush-hour

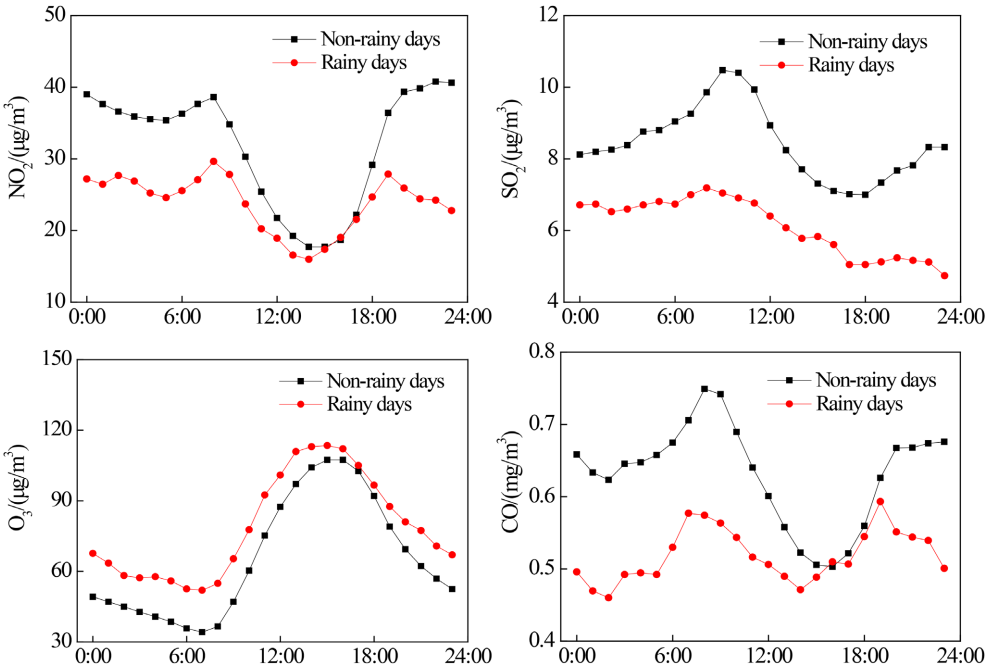


Figure 8. Diurnal variations in NO_2, SO_2, O_3, and CO mass concentrations on rainy and non-rainy days.

traffic emissions and nocturnal temperature inversions kept NO_2 concentrations high in the early morning and at night. Concentrations reached their daily minimum at 14:00, with a notable peak-to-trough difference. The SO_2 concentrations of 7.0 - 10.5 μg/m^3 followed a pattern with a single morning peak. After gradually increasing from early morning, the concentrations peaked at 9:00 and declined continuously, displaying clear diurnal fluctuations. As a typical photochemical pollutant, O_3 exhibited a single daytime peak, with concentrations varying in accordance with solar radiation intensity. A minimum concentration of 34.2 μg/m^3 at 7:00 contrasted with the maximum of 107.3 μg/m^3 from 15:00 to 16:00, resulting in a large day-night concentration difference. CO concentrations ranged from 0.5 to 0.7 mg/m^3 and were bimodal, with clear accumulation in the early morning and at night. The favorable atmospheric dispersion at noon reduced the concentrations to their minimum, contributing to a distinct contrast between daytime and nighttime concentrations.

On rainy days, conventional gaseous pollutants had lower overall concentrations and significantly reduced diurnal variability. NO_2 concentrations declined to 16.0 - 29.6 μg/m^3. Despite retaining a bimodal pattern, the concentrations had substantially lower peaks and smaller peak-to-trough differences, indicating that pollutant accumulation during both day and night was effectively reduced. The highly water-soluble SO_2 exhibited the greatest sensitivity to precipitation, with concentrations falling to 4.7 - 7.2 μg/m^3. Its original single peak almost disappeared, and the concentrations remained stable throughout the day (Zeng et al., 2021). CO concentrations of 0.5 - 0.6 mg/m^3 presented a less pronounced bimodal pattern and markedly weaker diurnal fluctuations. In contrast to these pollutants, O_3 concentrations increased on rainy days. Its minimum rose to 52.0 μg/m^3 and its peak reached 113.5 μg/m^3 at 14:00-15:00, with a broader peak and more prolonged high concentration. Two synergistic effects could explain this response. Precipitation removed atmospheric particles and enhanced solar radiation transmittance. In addition, the decline in atmospheric NO_2 concentrations reduced O_3 consumption through titration by nitrogen oxides. Together, these factors accelerated O_3 photochemical production. Convection-driven vertical mixing additionally transported O_3 downward from the lower stratosphere and upper troposphere, further increasing the near-surface concentrations (Yoo et al., 2014). Previous studies have found a more pronounced O_3 increase with nighttime precipitation than with daytime precipitation. O_3 is normally consumed through chemical reactions with vehicle exhaust components such as NO. Precipitation tends to decrease vehicle emissions and hence atmospheric O_3 consumption, resulting in higher O_3 concentrations than under non-rainy conditions (Wu et al., 2019).

Precipitation affected atmospheric pollutants differently. It primarily lowered the concentrations of conventional pollutants ($PM_{2.5}$, PM_{10}, NO_2, SO_2, and CO) through wet scavenging and improved atmospheric dispersion. PM_{10} and SO_2 were the most sensitive to precipitation. The $PM_{2.5}/PM_{10}$ ratio increased markedly because precipitation preferentially removed PM_{10}. Conversely, changes in

atmospheric composition and solar radiation increased O_3 concentrations. The findings demonstrate complex and pollutant-specific effects on the near-surface atmosphere. Accordingly, air pollution control should fully consider the multiple meteorological effects on pollutant concentrations and their composition.

4. Conclusion

1) Precipitation in the study area had a pH range of 6.18 to 8.02 and a volume-weighted mean of 6.71, indicating that precipitation was not acidified. For electrical conductivity, the range was 6.85 - 290 μS/cm, and the volume-weighted mean was 40.29 μS/cm. This value markedly exceeded that at the atmospheric background station, proving that anthropogenic activities significantly affected local precipitation.

2) The total ion concentrations in precipitation ranged from 86.14 to 3221.58 μeq/L, with a volume-weighted mean of 366.13 μeq/L, which was clearly above the background level. The cation composition was dominated by Ca^{2+} and NH_4^+, with volume-weighted mean concentrations of 100.03 and 54.12 μeq/L, respectively. These ions accounted for 46.82% and 25.33% of the total cations. The anion composition was dominated by NO_3^- and SO_4^{2-}, with volume-weighted means of 69.50 and 61.12 μeq/L and respective contributions of 45.57% and 40.08% to total anions. Overall, Ca^{2+}, NO_3^-, SO_4^{2-}, and NH_4^+ accounted for 77.78% of the total ions and constituted the predominant ionic components of local precipitation.

3) Compared with non-rainy days, the $PM_{2.5}$ and PM_{10} concentrations on rainy days were lower by 27.97% and 40.62%, respectively, whereas SO_2, NO_2, and CO concentrations were lower by 27.32%, 25.36%, and 17.78%, respectively. Precipitation exhibited clear wet scavenging effects on $PM_{2.5}$, PM_{10}, SO_2, NO_2, and CO. Compared with gaseous pollutants, particulate matter was removed more effectively, particularly its coarse fraction.

4) The effects of precipitation varied among atmospheric pollutants. The concentrations of $PM_{2.5}$, PM_{10}, NO_2, SO_2, and CO were reduced mainly through wet deposition and improved atmospheric dispersion, with PM_{10} and SO_2 showing the greatest sensitivity to precipitation. In contrast, O_3 concentrations increased on rainy days because of combined changes in atmospheric composition and solar radiation.

Funding

This research was funded by the Science Research Project of the Hebei Education Department (ZC2023015).

Conflicts of Interest

The authors declare no conflicts of interest regarding the publication of this paper.

References

Chen, P., Qu, X., Song, Z., Jia, Z., Zhang, F., & Cui, S. (2025a). Chemical Characteristics and

Source Apportionment of Water-Soluble Ions in Precipitation in Harbin, China. *Atmospheric Pollution Research, 16,* Article 102604. https://doi.org/10.1016/j.apr.2025.102604

Chen, X., Fan, H., Wang, X., Lou, Y., & Zhang, L. (2025b). Study on the Impact of Precipitation on Gaseous Pollutants in Dalian City. *Journal of Heilongjiang Vocational Institute of Ecological Engineering, 38,* 7-10+17. (In Chinese)

Cheng, X., & Huang, Y. (1998). A Classification Method to Analyze the Chemical Characteristics of Precipitation. *Climatic and Environmental Research, 3,* 83-89. (In Chinese)

Han, L., Zhang, H., Xiang, X., Zhang, P., Cheng, S., & Wei, W. (2017). Precipitation and Its Effects on Atmospheric Pollutants in a Representative Region of Beijing in Summer. *Environmental Science, 38,* 2211-2217. (In Chinese)

Hong, G., Zhou, J., Lan, Yali, Li, L., Feng, Y., & Yang, L. (2014). Characteristics and Cause Analysis on Acid Rain Pollution in Shijiazhuang City. *Hebei Journal of Industrial Science and Technology, 31,* 547-551. (In Chinese)

Hou, S. Y., Qiu, C. C., Ding, C., Wang, G. Z., & Yu, X. N. (2020). Analysis on Chemical Composition of Precipitation and Its Source Apportionment in Xi'an City. *Environmental Chemistry, 39,* 2384-2394. (In Chinese) https://doi.org/10.7524/j.issn.0254-6108.2020050501

Huang, X., & Li, S. Y. (2024). Economic and Industrial Development Significantly Contribute to Acidity and Ionic Compositions of Rainwater in China. *Water, 16,* Article 193. https://doi.org/10.3390/w16020193

Huang, Y. L., Yang, J. W., Liu, C., Jing, R. Y., & Lu, Q. H. (2024). Spatial and Temporal Variations in Rainwater Chemistry in a Rapid Urbanization Area of Shenzhen, China. *Atmosphere, 15,* Article 1536. https://doi.org/10.3390/atmos15121536

Li, L., Li, H., Peng, L., Li, Y., Zhou, Y., Chai, F., Mo, Z., Chen, Z., Mao, J., & Wang, W. (2020a). Characterization of Precipitation in the Background of Atmospheric Pollutants Reduction in Guilin: Temporal Variation and Source Apportionment. *Journal of Environmental Sciences, 98,* 1-13. https://doi.org/10.1016/j.jes.2020.03.029

Li, X., Zhao, L., Liu, Q., Zhao, Y., Cheng, J., Lu, J., & Zhao, P. (2020b). Chemical Composition of Precipitation and Its Sources in Shangluo City of Qinling Mountainous Area. *Journal of Water Resources & Water Engineering, 31,* 24-30. (In Chinese)

Lu, X., Li, L. Y., Li, N., Yang, G., Luo, D., & Chen, J. (2011). Chemical Characteristics of Spring Rainwater of Xi'an City, NW China. *Atmospheric Environment, 45,* 5058-5063. https://doi.org/10.1016/j.atmosenv.2011.06.026

Luan, Z., Lu, H., Li, T., Cui, X., Zhao, T., & Zhu, Q. (2021). Impacts of Precipitation and Wind on $PM_{2.5}$ Concentration and Its Region Transport in Tai'an. *Journal of Meteorology and Environment, 37,* 33-39. (In Chinese)

Si, L., & Li, Z. (2024). Atmospheric Precipitation Chemistry and Environmental Significance in Major Anthropogenic Regions Globally. *Science of the Total Environment, 926,* Article 171830. https://doi.org/10.1016/j.scitotenv.2024.171830

Sun, R., Li, X., Huang, H., Zhou, C., & Wang, Y. (2025). Influence of Meteorological Variables and Human Activities on Precipitation Chemistry in the Guanzhong Plain, Northwest China. *Atmospheric Pollution Research, 16,* Article 102523. https://doi.org/10.1016/j.apr.2025.102523

Sun, S., Liu, S., Li, L., & Zhao, W. (2021). Components, Acidification Characteristics, and Sources of Atmospheric Precipitation in Beijing from 1997 to 2020. *Atmospheric Environment, 266,* Article 118707. https://doi.org/10.1016/j.atmosenv.2021.118707

Tang, J., Xue, H. S., Yu, X. L., Cheng, H. B., Xu, X. B., Zhang, X. C., & Ji, J. (2000). The Preliminary Study on Chemical Characteristics of Precipitation at MT. Waliguan. *Acta Scientiae Circumstantiae, 20,* 420-425. (In Chinese)

https://doi.org/10.3321/j.issn:0253-2468.2000.04.008

Wang, B., Luo, X., Liu, D., Su, Y., & Wu, Z. (2021). The Effect of Construction Dust and Agricultural Fertilization on the Precipitation Chemical Composition during Summer in the Yangtze River Delta Area, China. *Atmospheric Pollution Research, 12,* Article 101121. https://doi.org/10.1016/j.apr.2021.101121

Wang, J., Hou, Q., Guo, R., Xu, M., Mao, N., Zhao, Y., Mao, Y., & Pang, Y. (2022). Chemical Composition of Precipitation and Its Scavenging Effect on Atmospheric Particulate Matter in Cangzhou City. *Journal of Cangzhou Normal University, 38,* 19-24. (In Chinese)

Wang, N., He, T., & Liu, J. (2017). The Scavenging Effect of Summer Precipitation on Atmospheric Pollutants in Chongqing Downtown. *Environmental Engineering, 35,* 69-73. (In Chinese)

Wu, G. F., Wang, L. L., Dong, J., Shen, N. C., Jiang, J. F., & Zhao, W. J. (2021a). Effects of Precipitation on the Removal of $PM_{2.5}$ and PM_{10} in Beijing Urban Area. *Environmental Monitoring in China, 37,* 83-92. (In Chinese) https://doi.org/10.19316/j.issn.1002-6002.2021.03.11

Wu, Y., Liu, W., Xu, Y., Xu, Z., Zhou, X., & Zhou, L. (2021b). Multiple Isotopic Tracing for Sulfate and Base Cation Sources of Precipitation in Hangzhou City, Southeast China: Insights for Rainwater Acidification Mechanism. *Environmental Pollution, 288,* Article 117770. https://doi.org/10.1016/j.envpol.2021.117770

Wu, Z., Wang, S., Song, D., Bai, H., & Li, H. (2019). Characteristics of Atmospheric Pollutants Concentration and Clearance of Precipitation in Guiyang City. *Plateau and Mountain Meteorology Research, 39,* 41-47. (In Chinese)

Xiao, Q., Han, L., Qi, C., Tian, J., Wang, H., Zheng, A., & Guo, J. (2024). Ionic Characteristics and Sources of Atmospheric Precipitation and Its Impacts on Environment at Typical Cities in China. *China Environmental Science, 44,* 5329-5343. (In Chinese) https://doi.org/10.19674/j.cnki.issn1000-6923.20240412.023

Xiao, Z. M., Li, P., Chen, K., Sun, R., Feng, Y., Liu, B., & Qiao, C. (2015). Characteristics and Sources of Chemical Composition of Atmospheric Precipitation in Tianjin. *Research of Environmental Sciences, 28,* 1025-1030. (In Chinese) https://doi.org/10.13198/j.issn.1001-6929.2015.07.02

Xiong, X., Zhang, W., Zhu, R., & Li, E. (2021). Influence of Precipitation on Mass Concentration of Atmospheric Pollutants in Cangzhou of Hebei Province. *Journal of Arid Meteorology, 39,* 296-301. (In Chinese)

Xu, Z., Li, Y., Tang, Y., & Han, G. (2009). Chemical and Strontium Isotope Characterization of Rainwater at an Urban Site in Loess Plateau, Northwest China. *Atmospheric Research, 94,* 481-490. https://doi.org/10.1016/j.atmosres.2009.07.005

Yang, F., Tan, J., Shi, Z. B., Cai, Y., He, K., Ma, Y. et al. (2012). Five-Year Record of Atmospheric Precipitation Chemistry in Urban Beijing, China. *Atmospheric Chemistry and Physics, 12,* 2025-2035. https://doi.org/10.5194/acp-12-2025-2012

Yang, J., Han, S., Yang, J., Wang, J., Liu, J., Tian, Y., Zhang, Y., Xue, P., Wang, Y., Zhao, Z., Chen, C., Cui, L., Yang, H., & Zhang, J. (2023). Seasonal Characteristics of Precipitation in Tianjin and Sources of Ion from Different Air Masses. *China Environmental Science, 43,* 1844-1856. (In Chinese)

Yoo, J., Lee, Y., Kim, D., Jeong, M., Stockwell, W. R., Kundu, P. K. et al. (2014). New Indices for Wet Scavenging of Air Pollutants (O_3, CO, NO_2, SO_2, and PM_{10}) by Summertime Rain. *Atmospheric Environment, 82,* 226-237. https://doi.org/10.1016/j.atmosenv.2013.10.022

Zeng, J., Ge, X., Wu, Q., & Zhang, S. (2021). Three-Year Variations in Criteria Atmospheric Pollutants and Their Relationship with Rainwater Chemistry in Karst Urban Region, South-

west China. *Atmosphere, 12,* Article 1073. https://doi.org/10.3390/atmos12081073

Zeng, J., Han, G., Wu, Q., Peng, M., Ge, X., Mao, S. et al. (2024). Chemical Evolution of Rainfall in China's First Eco-Civilization Demonstration City: Implication for the Provenance Identification of Pollutants and Rainwater Acid Neutralization. *Science of the Total Environment, 910,* Article 168567. https://doi.org/10.1016/j.scitotenv.2023.168567

Zhang, D. D., Jim, C. Y., Peart, M. R., & Shi, C. (2003). https://www.sciencedirect.com/science/article/abs/pii/S0048969702004643?via%3Dihub

Zhang, Q. (2013). The Influences of the pH of the Rain in Dalian Based on Multi-Step Sampling and Air Trajectory Clustering. *Arid Environmental Monitoring, 27,* 49-54. (In Chinese)